Design of the High-Precision Temperature Measurement System Integrated with Self-Heating Error Suppression Algorithm

***Abstract*—In temperature measurement applications using RTD. the selection of current amplitude and the system configuration have consistently been factors requiring a delicate balance. In order to enhance accuracy and reduce the impact of the self-heating effect. In this paper, Firstly, by calculating the parameters of current, circuit, and MCU configuration, multiple tests were conducted using the precision calibrator FLUKE 7625A to verify the system accuracy of the testing platform based on ADUCM360. it can achieve an accuracy of ±0.022°C within 0°C to +100°C. Then, by designing a thermal-electric-fluid coupled finite element simulation model, the self-heating effect and appropriate operational modes, are analyzed and calculated. The test results indicate that, with the application of the self-heating suppression algorithm in a 4-wire configuration using the PT100 (Platinum RTD Standard IEC 751 Class AA) for testing, in comparison to continuous operation mode, the maximum measurement error decreased from 0.0791°C to 0.0299°C, and the self-heating error is constrained within a range of ±0.006°C.**

I. Introduction

Temperature sensors are widely used in various fields such as industrial production, aerospace, medical devices, instrumentation, and other applications, Their accuracy, precision, and stability are crucial for the proper operation and safety of equipment. Due to its various advantages, RTD is one of the most commonly used industrial temperature measurement sensors. Its resistance changes with variations in ambient temperature. Because it is a passive device, It does not generate an output voltage on its own. To conduct resistance measurements, it is necessary to pass an external current through the resistor and measure the output voltage. Therefore, the selection of excitation current and resistors, wiring configuration, ADC operating mode, as well as the design of the measurement circuit, all bear critical importance in influencing the measurement accuracy of the system.

Among these factors, current is the most influential, as it can determine all other parameter settings. Increasing the excitation current can enhance the SNR of the input signal, and reduce resolution losses. However, due to the Joule heating effect, when current passes through a resistor, it generates heat, resulting in a temperature rise, commonly referred to as the self-heating effect. Inevitably, it introduces measurement errors, leading to inaccurate results. Taking into consideration factors such as the complexity and variability of current selection's impact on temperature measurement, The purpose of this work is based on the ADUCM360 to design a high-precision temperature measurement system and identify a method for eliminating or reducing self-heating errors caused by Joule heating.

By using a calibration source, the FLUKE 7625A, to verify system accuracy. In order to reduce the influence of the self-heating effect on measurement accuracy, commercial finite elements-based software Comsol Multiphysics v6.1 is utilized to model and simulate the temperature changes and distributions of an RTD. The simulation is based on thermal-electric-fluid coupled field analysis to compute the processes and distribution of heat conduction and temperature rise. Eventually, five different intermittent operating modes are designed, and experimental tests are conducted using simulation algorithms to validate their effectiveness.

II. Parameters Selection and Configuration of The Measurement System

RTD comes in various types, including PT100, PT200, PT500, PT1000, etc. Among these, PT100 is the most commonly used RTD. Therefore, this paper focuses on PT100, analyzing its application methods. Taking into account factors such as tolerance and measurement range, a wire wound class AA PT100 was chosen as the temperature sensor in this study.

There are several different wiring configurations available for connecting RTD to measurement devices, including 2-wire, 3-wire, and 4-wire configurations. Not only is the accuracy of the RTD itself a factor, but the resistance of the lead wires can introduce errors, particularly in long-distance applications. Therefore, in this paper, the 4-wire configuration is employed, which is relatively convenient in terms of its configuration, requiring only one current source, and it can provide the highest accuracy among these three configurations[1]. This is because the two wires carrying the excitation current are not part of the measurement circuit, and lead wire errors are not introduced into the measurement. The wires in the measurement circuit connect from the analog input terminals to both ends of the RTD. Considering the high input impedance of the ADC, there is almost no current flowing through the lead wires, resulting in minimal measurement error on the wires which nearly eliminates the lead wire errors. The 4-wire configuration is shown in Figure 1.

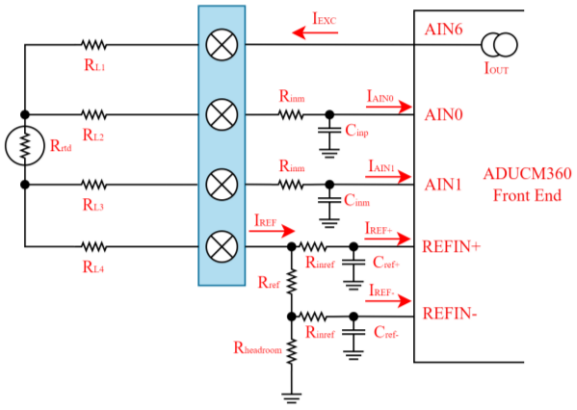

Fig 1. 4-wire configuration diagram

To achieve accurate temperature measurement, the system needs to have a sensor with a minimal tolerance, a matching circuit, the correct operating modes, appropriate measurement methods, and parameter selections to reduce measurement errors. In this paper, the ADUCM360 microcontroller which is commonly used in intelligent precision sensing systems and temperature measurement applications is chosen as the

measurement device. Its accuracy is validated by a precision calibration source, the FLUKE 7625A. Finally, Using a high-precision mercury thermometer as the reference standard, we conducted circuit parameters selection based on the measured temperature results.

A. Current selection

The selection of current plays a critically significant role in RTD temperature measurement applications, as the amplitude of the current directly determines various aspects within the ratiometric measurement circuit. These aspects encompass the reference resistor, headroom resistor, the operating mode of the ADC, including gain and filter configurations, as well as the operating modes of the current source.

The ADUCM360 provides multiple current output options ranging from 50uA to 1mA. Considering that passing a current through a resistor can introduce self-heating errors, many temperature measurement applications prefer to use lower current values, typically below 200uA or 100uA. However, using lower current values also presents several disadvantages, such as a decrease in temperature sensitivity and a reduction in the input signal SNR, leading to resolution loss. This is especially noteworthy for Σ-Δ ADC because increasing the gain will introduce additional noise from the PGA, where amplifier or thermal noise begins to dominate at high gains. Moreover, as the gain increases, both gain error drift and offset error drift also increase accordingly. However, selecting a higher current can effectively avoid these issues. Based on Figure 1, the following equations can be derived:

$$V_{MRTD}=V_{AIN0}-V_{AIN1} \tag{1}$$

$$V_{MRTD}=(I_{EXC}-I_{AIN1})\times R_{rtd}-(R_{inm}+R_{L1})\times(I_{AIN0}-I_{AIN1})$$

$$V_{REFIN}=(I_{REF}-I_{REF+})\times R_{ref}-R_{inref}\times(I_{REF+}-I_{REF-}) \tag{2}$$

$$R_{mrtd}=R_{ref}\times\frac{V_{MRTD}}{V_{REFIN}}=R_{ref}\times\frac{(I_{EXC}-I_{AIN0})\times R_{rtd}-(R_{inm}+R_{L})\times(I_{AIN0}-I_{AIN1})}{R_{ref}\times(I_{REF}-I_{REF+})-R_{inref}\times(I_{REF+}-I_{REF-})} \tag{3}$$

Where:

V_{MRTD} : the ADC analog input voltage

V_{REFIN} : the ADC reference input voltage

R_{mrtd} : The resistance value of the RTD measured using the ratio measurement method

R_{rtd}: The resistance value of the actual RTD

By simplifying equation (3), When $I_{AIN0}=I_{AIN1}$, $I_{REF+}=I_{REF}$. the following equation can be derived:

$$R_{MRTD}=R_{ref}\times\frac{I_{EXC}-I_{AIN0}}{I_{REF}-I_{REF+}}=R_{rtd}\times\frac{I_{EXC}-I_{AIN0}}{I_{EXC}-I_{AIN0}-I_{AIN1}-I_{REF+}} \tag{4}$$

It is evident that under the 4-wire configuration, increasing the excitation current while minimizing the input current at the measurement and reference terminals can improve accuracy and reduce the error between measured values and the actual PT100 resistance values.

B. MCU configuration

ADUCM360 is a microcontroller with an ARM Cortex-M3 core that incorporates dual 24-bit multichannel Σ-Δ ADCs PGAs and buffers. To reduce the error and meet the precise measurement requirements, choosing an appropriate gain to amplify the input signal becomes crucial. This is crucial for effectively utilizing the dynamic range of the ADC and minimizing quantization errors. However, it's important to be aware that as the gain increases, the offset error drift, the gain error drift, and the integral nonlinearity also increase simultaneously. When the gain ≥ 16, the INL can reach ±20ppm of FSR and the gain error drift can reach ±6ppm/°C.

As the temperature measurement range is from 0°C-100°C, the resistance of PT100 varies between 100Ω-138.5Ω and the ADUCM360 provides multiple current output options ranging from 50uA to 1mA. According to the datasheet[2], the input voltage range also varies with the gain and it is also correlated with the selection of current. If the system's minimum resolution needs to be at least 0.1°C, When using an excitation current of 1mA, The noise-free resolution for the measurement system is shown in equation (5). The resolution loss and the minimum required system resolution derived from the datasheet are shown in equations (6) and (7).

$$\text{noise-free resolution}=\log_2\left(\frac{100°C-0°C}{0.1°C}\right)=9.96\text{bits} \tag{5}$$

$$\text{Resolution loss}=\log_2\left(\frac{(\text{Resistance variation range})\times\text{Gain}\times I_{EXC}}{2\times V_{ref}}\right) \tag{6}$$

$$\text{System-required resolution} = 9.96-\text{Resolution loss} \tag{7}$$

Based on the input voltage range and the excitation current, when the reference voltage is 2.5V, using the system's chopping feature with sinc3 filter, the system-required resolution can be calculated, achieving a resolution of 0.1°C is possible only if it is less than the peak-to-peak resolution from the datasheet of ADUCM360 which is shown in Tables 1 and 2. However, when using a lower current, it becomes imperative to apply a higher gain; otherwise, the 24-bit Σ-Δ ADC of ADUMC360 may fail to meet the resolution requirement or does not have a sufficient margin which can also lead to an increase in gain error and offset error, resulting in inaccurate measurements.

TABLE 1. SYSTEM REQUIRED RESOLUTION

Iexc(uA)	The system required resolution by different Gains and Currents			
	Gain=1 (19.4p-p)	Gain=2 (18.2p-p)	Gain=4 (18.1p-p)	Gain=8 (17.7p-p)
1000	16.9809	15.9809	14.9809	
800	17.3029	16.3029	15.3029	14.3029
750	17.3960	16.3960	15.3960	14.3960
600	17.7179	16.7179	15.7179	14.7179
500	17.9809	16.9809	15.9809	14.9809
450	18.1329	17.1329	16.1329	15.1329
400	18.3029	17.3029	16.3029	15.3029
300	18.7179	17.7179	16.7179	15.7179
250	18.9809	17.9809	16.9809	15.9809
200	19.3029	18.3029	17.3029	16.3029
150	19.7179	18.7179	17.7179	16.7179
100	20.3029	19.3029	18.3029	17.3029
50	21.3029	20.3029	19.3029	18.3029

TABLE 2. SYSTEM REQUIRED RESOLUTION

Iexc(uA)	The system required resolution by different Gains and Currents			
	Gain=16 (17.7 p-p)	Gain=32 (16.9 p-p)	Gain=64 (15.7 p-p)	Gain=128 (15.1 p-p)
1000				
800				
750				
600				
500				
450	14.1329			
400	14.3029			
300	14.7179			
250	14.9809			
200	15.3029			
150	15.7179	14.7179		
100	16.3029	15.3029		
50	17.3029	16.3029	15.3029	14.3029

When the gain ≤ 16, the Offset Error Drift, Gain Error Drift, and Integral Nonlinearity are all identical, furthermore, when the system's chopping feature is employed with a gain of 4, its minimum Power Supply Rejection can reach 95dB. Taking into account that when Gain=4 and the excitation current is 1mA, it requires at least 14.98 bits which is less by 3.12 bits than what the system can provide.

In a typical working environment, temperature changes are very slow and can be considered as linear variations. Within a relatively short time duration, it can be treated as a DC signal. therefore, there isn't a high demand for a high sampling rate. Therefore, this paper selects the gain=4 configuration for the measurement. simultaneously, enabling system chopping, Sinc3 filter, and notch feature are commonly used for 50 Hz/60Hz rejection, which can also significantly reduce offset error and drift and support a maximum sampling rate of 488Hz, well exceeding the requirements of temperature measurement applications.

ADUCM360 offers four calibration modes to reduce the gain and offset errors. During the gain calibration, whether it is the internal or system calibration, the gain needs to be set to 1. And the system zero-scale calibration requires shorting external input pins. Therefore, to simplify the calibration process after each power-up, the internal gain calibration and internal offset calibration are chosen. Considering that the typical value of the offset error is 1uV when enabling system chopping, the calibration process can effectively control the offset error within a very low range.

C. Measurement circuit configuration

From the ADUCM360 datasheet, when the output current is greater than or equal to 50uA, the typical initial tolerance value at 25℃ can reach ±5%. Due to the relatively large output error of the current source, employing a common-voltage reference as the reference source may result in a measurement error of up to 17.98℃ in the worst case. This is an unacceptable result for measurement applications. This is the reason why the ratiometric measurement method is needed, as it can eliminate errors caused by the current source. The equation is shown below：

$$R_{MRTD}=R_{ref}\times\frac{V_{rtd}}{V_{ref}} \quad (8)$$

From Equation (8), it can be observed a high-precision reference resistor can reduce measurement errors from the temperature coefficients and the tolerance. Considering the targeted measurement range is from 0 to 100°C, with an external excitation current of 1mA, and along with the required external reference voltage input range specified in the datasheet, in order to minimize the input leakage current, a resistor with a tolerance of 0.1%, a temperature coefficient of 5ppm/°C, and a resistance value of 2.5kΩ is chosen as the external reference resistor.

In order to reduce the reference input current and minimize the gain error of the ADC, it is necessary to enable the buffered mode where the typical input current is only 4nA, significantly lower than that in the unbuffered mode. Furthermore, the absolute voltage input range of the reference is from AGND + 0.1V to AVDD − 0.1V. To ensure that the reference voltage does not exceed the tolerance input range, A headroom resistor needs to be connected in series between the reference resistor and the ground. Since the excitation current is 1mA, the resistance value of the headroom resistor is at least 100Ω. Considering the need for voltage margin, in this paper, a resistor with a tolerance of 0.1%, a temperature coefficient of 5ppm/°C, and a resistance value of 150Ω is chosen as the headroom resistor. The following table presents all the configuration details of ADUCM360.

TABLE 3. THE CONFIGURATION OF MEASUREMENT SYSTEM

Parameter	Configuration
Reference mode	External reference buffered mode
Gain calibration	Internal full-scale calibration
Offset calibration	Internal zero-scale calibration
Headroom Resistor	150Ω(0.1% 5PPM/℃)
Reference Resistor	2.5kΩ(0.1% 5PPM/℃)
Filter	Sinc3
Reference voltage	2.5V
Current	1mA
Gain	4

III. SYSTEM ACCURACY MEASUREMENT AND COMPARISON

The system design, which includes circuit parameters selection and MCU configurations, has been completed through theoretical analysis and calculations. A temperature measurement system requires a high-precision reference source to validate its measurement accuracy and errors. Therefore, The Fluke Calibration 7526A Precision Process Calibrator has been chosen as the reference source which can simulate the RTD resistance variations. When setting the temperature in PT100 mode, it can output the corresponding resistance value at the selected temperature. This instrument is commonly utilized for calibrating RTD, thermocouples sensors, temperature, and pressure process instrumentations and Its accuracy in the PT385-100 mode remains within ±0.02°C over the course of one year within the equivalent temperature range of -80°C to 100°C.

A. System Accuracy Test by FLUKE 7526A

To ascertain whether the utilization of a higher current is beneficial in enhancing measurement accuracy in the temperature measurement application of the ADUCM360. In the controlled experimental group, a reference resistor with a resistance value of 50kΩ, a tolerance of 0.1%, and a temperature coefficient of 5ppm/°C, as well as a headroom

resistor with a resistance value of 3kΩ, a tolerance of 0.1%, and a temperature coefficient of 5ppm/°C, were used with an excitation current of 50μA.

Connect the calibration source to the temperature measurement circuit as shown in Figure 2. Record the output temperature from the Fluke 7625A and the temperature readings obtained from the ADUCM360 temperature measurement system separately. Consider the readings from the Fluke 7625A as the reference values, and treat the ADUCM360 readings as measurement values. The difference between them represents the measurement error of the ADUCM360 system, which can be calculated using the formula shown in Equation (9).

$$T_{error}=T_{7625A}-T_{ADUCM360} \quad (9)$$

Where:

T_{error} : the temperature measurement error of ADUCM360.

T_{7625A} : the equivalent output temperature of FLUKE7625A.

$T_{ADUCM360}$: The reading value of ADUCM360.

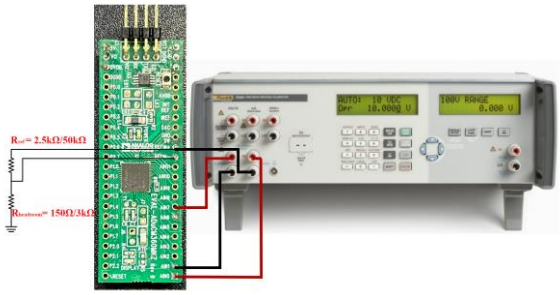

Fig 2. Measurement connection diagram

In the equivalent temperature range of 0°C -100°C, a total of 11 measurement points have been selected which are 0°C, 10°C, 20°C, 30°C, 40°C, 50°C, 60°C, 70°C, 80°C, 90°C, and 100°C, respectively.

In the measurement experiments, there are 4 different ADUCM360 selected to test their measurement accuracy. Among these, three of them used an excitation current of 1mA, while one used an excitation current of 50uA. At each testing point, a minimum of 60 tests were conducted. The error results figure for each part is shown below.

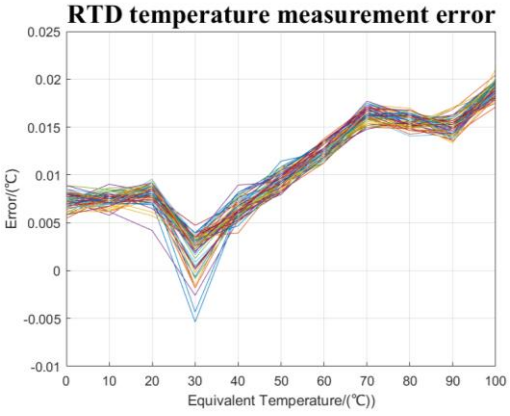

(a)

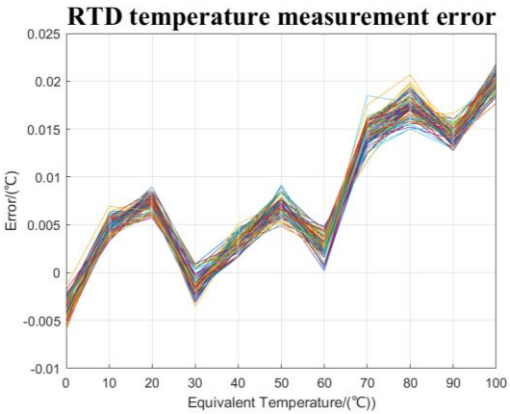

(b)

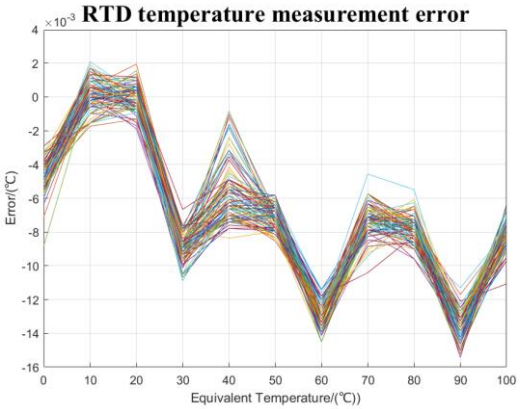

(c)

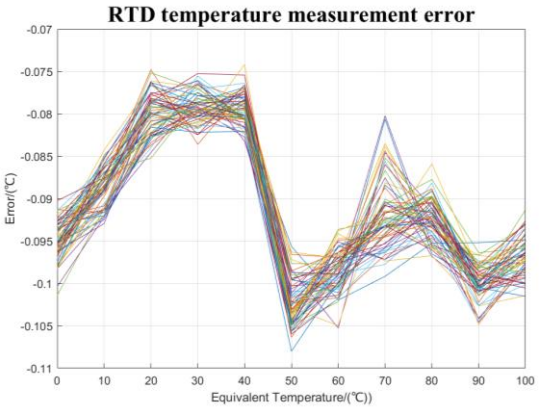

(d)

Fig 3(a). EVB1, Measurement error of 1mA (b). EVB2, Measurement error of 1mA (c). EVB3, Measurement error of 1mA .(d) EVB4, Measurement error of 50uA

From the above figures, it can be observed that when the excitation current is 1mA, the maximum measurement error does not exceed 0.023°C. When the excitation current is 50uA, the minimum measurement error is not less than 0.074°C. Based on the ADUCM360 evaluation design CN-0221, using the 1433-Z decade resistor to simulate an RTD resistor with an excitation current of 200uA, within the equivalent temperature range of 0°C to 100°C, the minimum error is not less than 0.05°C.

B. Test with Class AA PT100

The previous experiments indicate that using a higher current for measurement can effectively reduce system errors.

However, factors related to self-heating effects or self-heating errors have not been taken into account. Therefore, in the subsequent steps, a wire-wound class AA PT100 is connected to the measurement circuit to measure the temperature of water in an indoor environment. Since water has the highest specific heat capacity among common materials, it can ensure the stability of the ambient temperature. A high-precision mercury thermometer with an accuracy of 0.01°C and a range of 22°C-27°C is selected as the reference. The readings from the ADUCM360 are considered as the measured values. The difference between the two represents the error of the overall temperature measurement system after connecting the PT100.

10 tests were performed at 1mA excitation current, each test lasting 200s with a sampling rate of 0.5sps. The measurement error results are shown in the following graph.

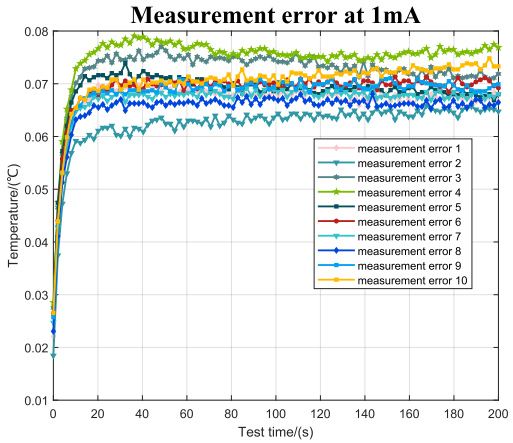

Fig 4. Measurement error at 1mA

It can be observed that a noticeable self-heating effect occurs when using a 1mA current. The self-heating errors were calculated by subtracting the initial measurement results from each subsequent measurement result, as shown in the following figure.

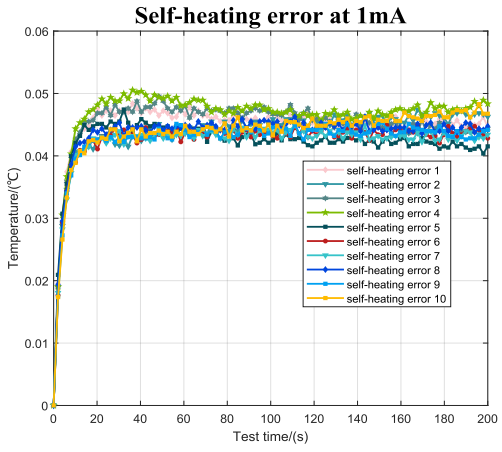

Fig 5. Self-heating error at 1mA

Based on Figures 4 and 5, within an ambient temperature range of 23°C-25°C, the maximum measurement error does not exceed 0.08°C. Thermal equilibrium is typically reached after about 20 seconds of testing. After that, the minimum self-heating error remains greater than 0.04°C but still below 0.051°C. When using a 50uA current, the measurement errors and the self-heating errors are shown in the following figures.

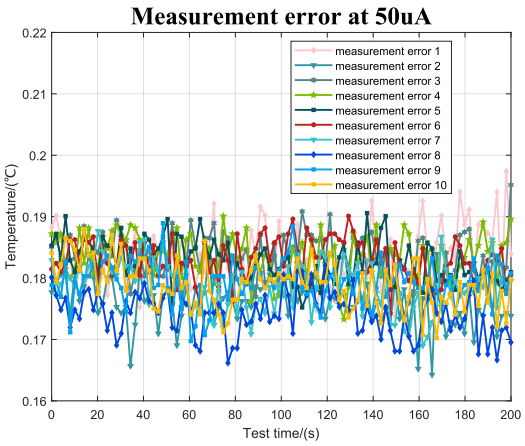

Fig 6. Measurement error at 50uA

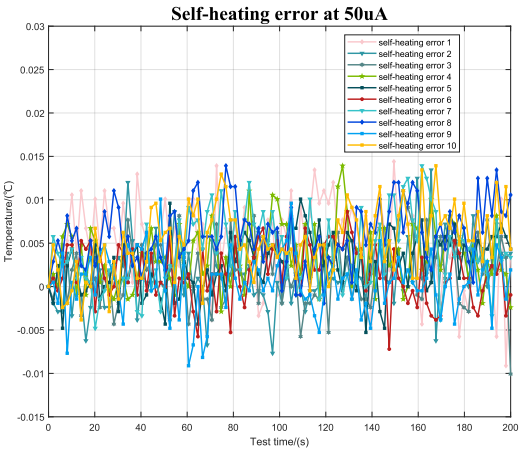

Fig 7. Self-heating error at 50uA

From Figures 6 and 7, within an ambient temperature range of 23°C-25°C, the maximum measurement error can reach 0.196°C. the minimum measurement error is still greater than 0.16°C which is significantly greater than the maximum measurement error obtained using 1mA current. This also validates the outcomes during system measurements. It can be observed that when using a 50uA current. The self-heating effect is not pronounced, and the heating effect error ranges within ±0.015°C which is only around 1/3 of the 1mA self-heating error.

IV. Simulation Model Design and Validation

Based on the previous analysis, Using a high current for temperature measurement yields higher measurement accuracy compared to a low current. However, there is a clear presence of self-heating error. If it is possible to reduce and eliminate self-heating errors through the design of different operational modes with corresponding algorithms, this holds certain engineering significance for improving the accuracy of the system.

The numerical analysis of the self-heating effect in PT100 involves a multi-physics coupling computation that combines electromagnetic fields, fluid dynamics, and temperature fields. Using finite element analysis software to analyze the temperature distribution and variations within the PT100 can help reconstruct temperature variations in the time domain and facilitate the development of corresponding algorithms.

A. Principles and Governing Equations

a) Electric field

The Computation of the self-heating error in PT100 involves the solution of a time-independent temperature field. wherein the heat source, the PT100 resistance value, varies with time and temperature. It adheres to the standardized relationship between temperature and resistance outlined in the IEC 60751 standard, which exhibits near linearity within the typical measurement range, particularly in the range of 0°C to 100°C, where the resistivity temperature coefficient of platinum is equal to 0.00385Ω/°C. The relationship is expressed as the equation below which can be used in the electric current field as the governing equation:

$$R_{rtd}(T)=R_0\times(1+\alpha T) \tag{10}$$

Where:

T: the ambient temperature(℃).

R_0: Rated Resistance at 0°C(100 Ω).

$R_{rtd}(T)$: Resistance of RTD at ambient temperature.

α = 0.00385Ω/°C.

b) Temperature field

For a PT100, Joule heating is generated due to the excitation current, and this heat varies with time and resistance, causing a corresponding temperature change. In the scenario of measuring water temperature, There is heat transfer in solids where conduction dominates and heat transfer in fluids where convection usually dominates. In thermal conduction, heat flow in solids refers to the movement of heat from regions of higher temperature to regions of lower temperature, including the porcelain substrate, alumina insulation powder, stainless steel sheath, and platinum wire. Thermal convection refers to the heat exchange that occurs between water and the air within the porcelain insulator as they come into contact with the surrounding solid. The heat transfer processes can be expressed as follows:

$$\rho c_p \frac{\partial T}{\partial t}+\Delta\cdot\left(\rho c_p \mathbf{u} T\right)-\nabla\cdot(k\nabla T)=Q+Q_{ted} \tag{11}$$

Where:

c_p: The Specific heat capacity of fluid.

$\boldsymbol{u}$: The Fluid velocity vector, u(x,y,z).

ρ: The fluid density.

k: The heat transfer coefficient.

Q: Volumetric heat generation.

Q_{ted}: external heat sources (self-heating effect).

c) Fluid field

In the scenario, the temperature of the stagnant liquid is measured by a stationary sensor. Therefore, it is permissible to entirely disregard the viscosity effect and turbulent flow. it can be regarded as natural convection. both the flow of air inside the porcelain substrate and the flow of water surrounding the PT100 externally adhere to the principle of conservation mass and momentum conservation which can be expressed as follows:

$$\rho\frac{\partial \mathbf{u}}{\partial t}+\rho(\mathbf{u}\cdot\nabla)\mathbf{u}=\nabla(-\rho\mathbf{I}+\mathbf{K})+\mathbf{F} \tag{12}$$

$$\frac{\partial p}{\partial t}+\nabla\cdot(\rho\mathbf{u})=0 \tag{13}$$

$$\mathbf{K}=\mu(\nabla\mathbf{u}) \tag{14}$$

Where:

u: The Fluid velocity vector.

F: The volume force density.

I: Identity matrix.

K= The Fluid vorticity vector.

ρ: The fluid density.

p: The fluid pressure.

μ: The fluid dynamic viscosity.

In experiments where temperature variations are minimal, the density of air and water remains essentially unchanged, and thus they can be treated as incompressible fluids.

B. Design of the simulation

a) Physical model and material properties

The simplified simulation model are shown in the figures below, with the PT100 model designed based on the actual construction. It includes a stainless steel sheath, alumina insulation powder, and porcelain substrate, platinum coil. The stainless steel sheath has a height of 26 mm and a diameter of 11mm. The alumina insulation powder has a height of 25 mm and a diameter of 10 mm. The porcelain substrate has a height of 23.5 mm and a diameter of 9 mm. The diameter of the platinum coil is 0.0008 inches, while the common coil diameters typically range from 0.0005-0.0015 inches.

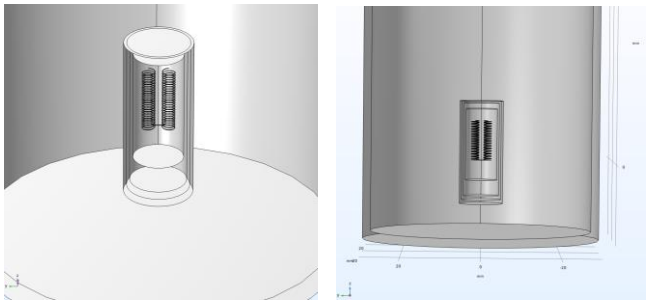

(a) (b)

Fig 8. Geometric model

When analyzing the self-heating effect, only the resistance parameters of the platinum coil are set as a function of temperature to better represent the self-heating effect of PT100 and improve the accuracy of the computed results, as shown in equation (10). Considering its low heat generation and the fact that other components such as the stainless steel sheath are not included within the measurement circuit, the temperature rise has a minimal impact on the material properties of the other components, the heat conduction, and thermal convection processes within the PT100. Therefore, the material properties of the other components can be considered constant. The physical properties of fluid materials are shown in Table 4, and the physical properties of solid materials are shown in Table 5.

TABLE 4. PHYSICAL PROPERTIES OF FLUID MATERIALS

Parameter	Air	Water
Density /(kg·m^{-3})	1.225	997
Specific heat capacity J/(kg·K)	1005	4186
Heat Conductivity W/(m·K)	0.0257	0.606
Viscosity /(Pa·s)	1.79×10^{-5}	0.001

TABLE 5. PHYSICAL PROPERTIES OF SOLID MATERIALS

Parameter	Porcelain	Stainless steel	Alumina
Density /(kg·m^{-3})	2500	7850	3965
Specific heat capacity J/(kg·K)	837	475	730
Heat Conductivity W/(m·K)	2	44.5	35

b) Boundary conditions and computational mesh

In the simulation model established in this paper, the following boundary conditions were set: the initial ambient temperature was set to 24.6°C, and the atmospheric pressure was 101.3kPa. No-slip condition is considered in the contact surface between fluid and the solid surface in the container except for the surface between air and water.

Due to the air gap between the platinum coil and the porcelain substrate within the PT100. Therefore, it is necessary to divide the inner air area more finely when meshing which aids in providing a clearer representation of the temperature gradient characteristics within the PT100 and the temperature variations at the fluid-solid boundary. It is meshed with a free tetrahedral grid of 376796 elements. When it comes to meshing the platinum coil, it is important to pay attention to the issue of computational convergence. Because of its minimal diameter, using free tetrahedral meshing requires many computational elements, demanding significant computational resources and time, and may even render the computation infeasible. On the other hand, an insufficiently fine meshing could result in numerous low-quality elements, potentially leading to error. Therefore, using the swept mesh functionality to mesh the coil becomes the only option. The coil is meshed with a swept grid of 1000 elements. As shown in figure 9.

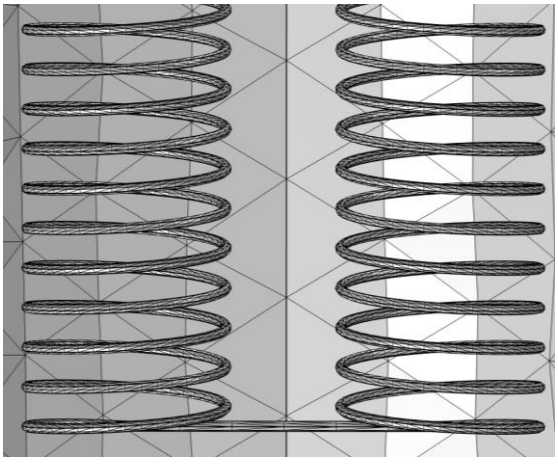

Fig 9. Computational mesh of the coil

C. Model Validation

Since in the previous sections. the results of ten measurements have been presented along with the self-heating error of the PT100 within the ambient temperature range of 23℃-25℃. After calculating their average value, the results are compared to the maximum simulated temperature value of the PT100 which is shown in figure 10. The maximum error does not exceed 0.003℃. the temperature distribution is shown in figure 11.

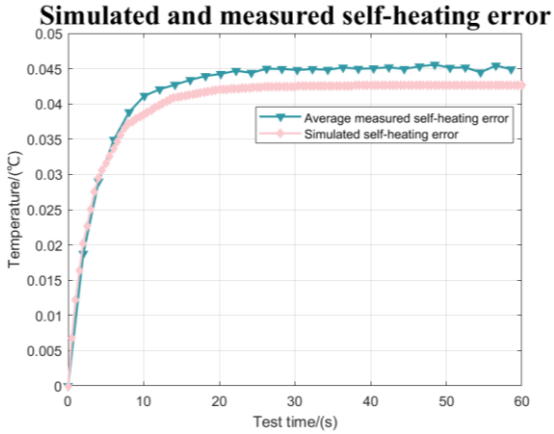

Fig 10. Comparison of the simulated and measured result using 1mA

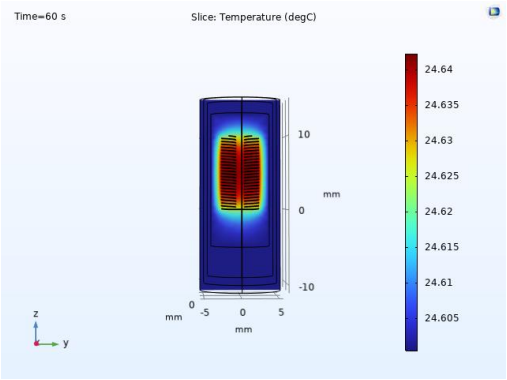

Fig 11. Temperature Distribution of PT100 in the 60s

When the initial simulated environmental temperature is 0°C, By varying the excitation current values and calculating, multiple temperature curves can be obtained which is shown in Figure 11(a). The relationship between the temperature change after reaching thermal equilibrium and the excitation current values is shown in Figure 11(b). This relationship, as mentioned in the article[3], also validates the accuracy of this model. The maximum error between those two simulation models does not exceed 0.025℃.

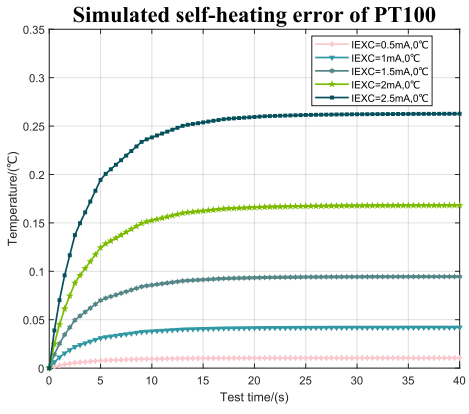

(a)

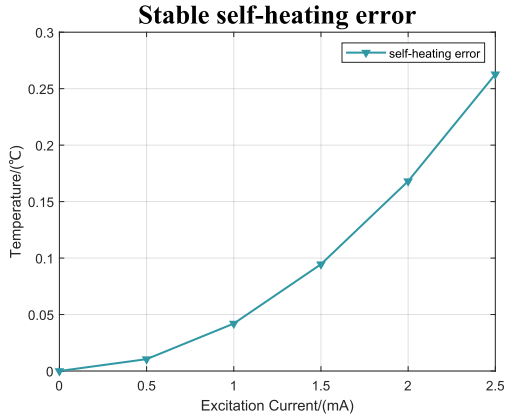

(b)

Fig 11(a). Self-heating error for different excitation currents (b). Stable self-heating error

VI. Algorithm And Test

It is clear that the simulation model designed in this paper can reasonably accurately reproduce the self-heating temperature-rising process, the accuracy that has been verified through comparative analysis and experimental tests. However, in practical applications, it is noteworthy that the current source is not continuously turning on. This introduces a significant concern leading to pronounced self-heating effects. Consequently, using intermittent modes provides a viable solution to address these issues. Therefore, In the subsequent sections, there will be a discussion on how to design operational modes and their corresponding algorithms, as well as the system's accuracy.

A. Algorithm Development

To accommodate diverse sampling rate requirements, this paper has designed five different intermittent modes. Among these, Mode 1 corresponds to a sampling period of 1.6s. Mode 2 to a sampling period of 5.6s. Mode 3 to a sampling period of 10.6s. Mode 4 to a sampling period of 15.6s. and Mode 5 to a sampling period of 20.6s. The duration for which the current source is turned on and off can be observed by the oscilloscope, as shown in Figure 12. Corresponding algorithms are designed based on the actual variation process.

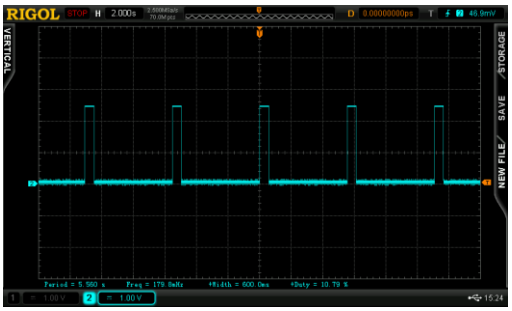

Fig 12. Variation of current

Using the event interface in COMSOL Multiphysics v6.1 can be effective in solving time-dependent models, enabling the definition of a set of discrete variables that exhibit discontinuity over time. This approach is especially well-suited for simulating periodic on/off switching conditions. Based on the five different operational modes, the simulated self-heating errors are computed when the excitation current is set at 1mA, 500uA, and 250uA, as depicted in Figure 13.

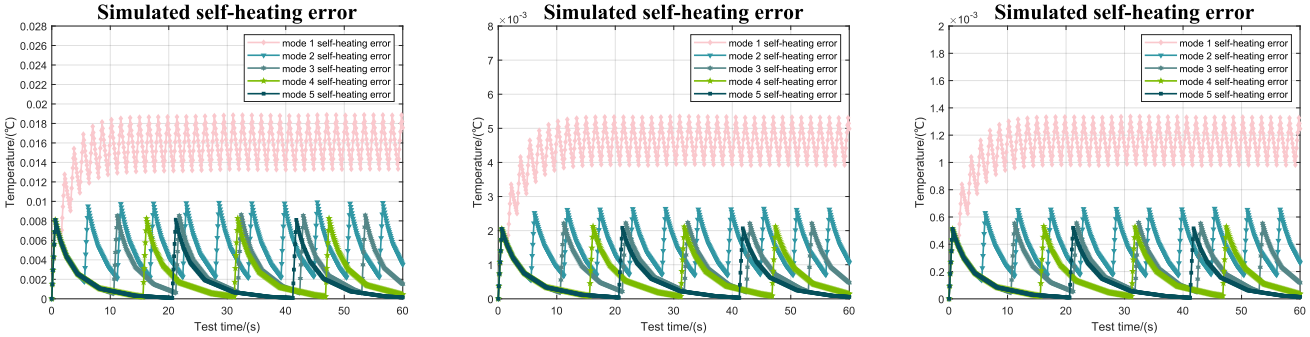

(a) (b) (c)

Fig 13(a). Simulated self-heating error (I_{EXC}=1mA) (b). Simulated self-heating error (I_{EXC}=500uA) (c). Simulated self-heating error (IEXC=250uA)

When an excitation current of 1mA is used, the envelope function formed by fitting the maximum self-heating error within each cycle from Mode 1 through Mode 5 is shown below:

$$T_{shem1} = 0.01834\times e^{0.0005876t} - 0.01702\times e^{-0.5313t} \quad (14)$$

$$T_{shem2} = 0.00967\times e^{0.0004352t} - 0.009659\times e^{-2.959t} \quad (15)$$

$$T_{shem3} = 0.00856\times e^{0.0001115t} - 0.00855\times e^{-4.336t} \quad (16)$$

$$T_{shem4} = 0.00835\times e^{0.0000262t} - 0.008327\times e^{-4.533t} \quad (17)$$

$$T_{shem5} = 0.00835\times e^{0.000317t} - 0.008329\times e^{-4.376t} \quad (18)$$

Where:

T_{shemx}: The self-heating error under mode x.

t: The sample duration.

B. Accuracy tests using the compensation algorithm

To implement the self-heating error suppression functionality. the error functions in the ADUCM360 should be written into it. Alternatively, the peak-to-peak values within each sampling period can also be written into the ADUCM360. And, based on the sampling duration, The compensated measurement error is calculated according to the following formula.

$$T_{error} = T_{measured} - T_{self\text{-}heating\text{-}simulated} - T_{true} \quad (19)$$

Where:

T_{error}: The error after the algorithm compensation.

$T_{measured}$: The measurement value of ADUCM360.

$T_{self\text{-}heating\text{-}simulated}$: The self-heating error calculated by the simulated model.

T_{true}: The temperature measured by the thermometer.

After adding the self-heating suppression algorithm into the ADUCM360, a total of 30 sets of temperature measurement experiments were conducted, with 6 measurements performed for each mode. The measurement errors are shown in the following figures.

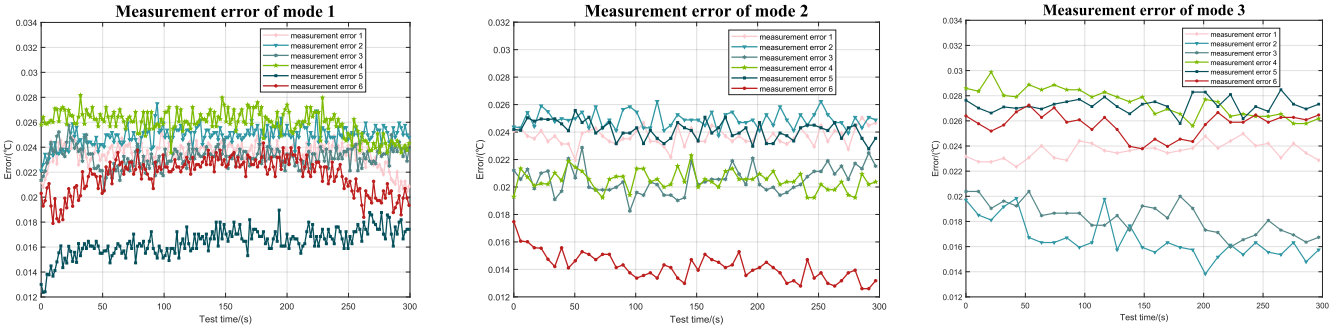

(a) (b) (c)

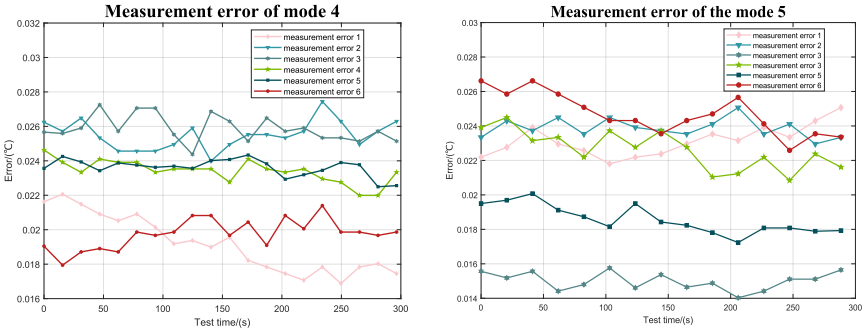

(d) (e)

Fig 13(a). Measurement error of mode 1 (b). Measurement error of mode 2 (c). Measurement error of mode 3 (d). Measurement error of mode 4 (e). Measurement error of mode 5

It can be observed that the algorithm effectively reduces measurement errors, with the maximum error not exceeding 0.03℃ across all the 5 modes. In order to analyze the suppression effect of the algorithm on self-heating error. It can be defined that the self-heating errors were calculated by subtracting the initial measurement errors from each subsequent measurement errors, as shown in the following figures.

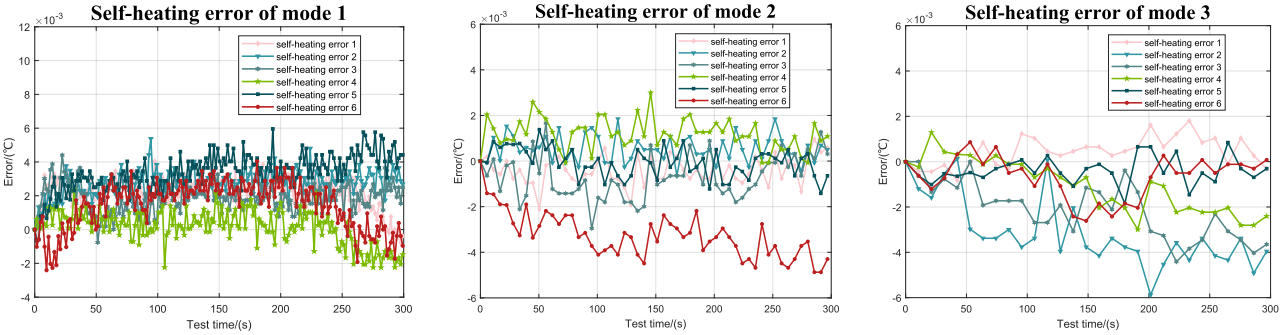

(a) (b) (c)

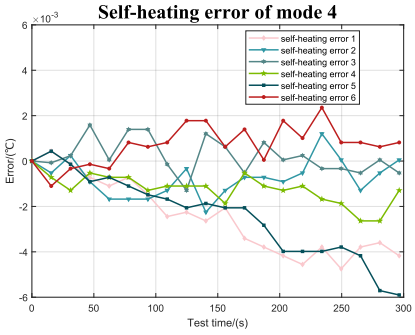

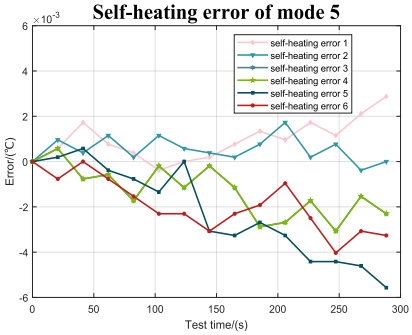

(d) (e)

Fig 14(a). Self-heating error of mode 1 (b). Self-heating error of mode 2 (c). Self-heating error of mode 3 (d). Self-heating error of mode 4 (e). Self-heating error of mode 5

From the above context, it can be observed that when the excitation current is equal to 1mA, the self-heating error after thermal equilibrium is between 0.04℃-0.051℃. when the self-heating error suppression algorithm is applied, in model 1, the self-heating error essentially falls within the range of -0.003℃ to 0.006℃. In modes 2,3,4 and 5, the self-heating error generally remains within the range of -0.006℃ to 0.003℃. Thus, it can be considered that the self-heating error is within ±0.006℃. This represents an obvious reduction in errors compared to the measurements obtained without the use of the algorithm, the self-heating errors have significantly decreased. This not only preserves the advantage of improving measurement accuracy by using higher current but also significantly reduces measurement errors caused by the self-heating effect.

VII. Conclusion

This paper focuses on the temperature measurement design of ADUCM360 and the temperature distribution computation of the PT100 by 3-D electrical-thermal-fluid analysis. The accuracy of the temperature measurement system has been demonstrated through actual tests. it can achieved an accuracy of ±0.022°C within 0°C to +100°C, as verified by Fluke 7625A. Moreover, the self-heating effect, the electrical and thermal properties of PT100 are analyzed by coupled analysis. When using a class AA PT100 with a 4-wire configuration, comparing the measurement results obtained by using the self-heating suppression algorithm in intermittent modes to those obtained in the continuous mode, The maximum measurement error decreased from 0.0791°C to 0.0299°C, and the self-heating error falls within the range of ±0.006°C.

References

[1] Jellenie Rodriguez and Mary McCarthy.” How to Select and Design the Best RTD Temperature Sensing System” Analog Dialogue, Vol 55, No. 2, JUN, 2021.

[2] ADUCM360 Data Sheet, Analog Devices, Inc.

[3] P. S. M. Saad, A. Ahmad and H. Hashim, "Determination of Excitation Current Range to Reduce Self-Heating using LTSpice for Resistance Temperature Detector in Aircraft System," 2023 IEEE 3rd International Conference in Power Engineering Applications (ICPEA), Putrajaya, Malaysia, 2023, pp. 185-190, doi: 10.1109/ICPEA56918.2023.10093215.

About the Authors

Leon Yan is an applications engineer in the Central Application Center at Analog Devices. Leon joined Analog Devices in 2022 after graduating from Chongqing University with a master’s degree in electrical engineering. He is interested in history and art.

Karl Wei joined ADI in 2000 and is now a system applications manager with the China Central Applications Team. His area of expertise is precision signal chains in industrial applications. Prior to that, he worked in IC test development engineering and marketing for 8 years. In 1992, he graduated with an M.S.E.E. from Harbin Institute of Technology, China.